Available online at www.sciencedirect.com
SCIENCE DIRECT®

Journal of the European Ceramic Society 23 (2003) 1243–1255
www.elsevier.com/locate/jeurceramsoc

Quantitative X-ray diffraction analysis of reactive infiltrated boron carbide–aluminium composites

Gürsoy Arslan*, Ferhat Kara, Servet Turan

Anadolu University, Department of Materials Science and Engineering, Iki Eylül Kampüsü, 26555 Eskisehir, Turkey

Received 1 March 2002; received in revised form 12 August 2002; accepted 19 August 2002

Abstract

Dense (> 98% of theoretical) boron carbide (B_4C)–aluminium (Al) composites were produced between 985 and 1370 °C by pressureless melt infiltration of Al alloys into porous B_4C compacts under argon (Ar) atmosphere. The microstructure of the composites were investigated using a scanning electron microscope (SEM) and the phases were determined quantitatively by the ratio of slopes method using X-ray diffraction (XRD) analysis. XRD results showed that B_4C–Al composites are composed of various combinations of Al_3BC, AlB_2, $AlB_{12}C_2$ and Al_4C_3 phases. The type of phases formed and their quantities depend on processing conditions. The AlB_2 phase forms at relatively small amounts and its formation can be significantly suppressed or totally eliminated by increasing the particle size of the starting B_4C powder and/or altering its surface chemistry. The Al_3BC phase, on the other hand, is observed to be the main reaction product forming and is always present in all composites. The other phases, $AlB_{12}C_2$ and Al_4C_3, are observed to form only at the higher end of the investigated temperature interval. The formation of hygroscopic Al_4C_3 phase necessitates a prolonged exposure in addition to high temperatures. Coating the surface of the starting B_4C powder with SiO_2 or passivating reduces the amount of reaction products substantially. Infiltration of B_4C by Al is assisted by the formation of Al_3BC.

Keywords: B_4C; Al; Infiltration; Wetting; X-ray methods

1. Introduction

Monolithic B_4C ceramic is a low-density material that is very hard, strong and stiff. However, densification of monolithic B_4C requires high temperatures and/or application of high pressures.[1] Another major limitation to its widespread use arises from its extreme susceptibility to brittle fracture. Researchers have known that combining B_4C with a metal could solve the recognized difficulties with B_4C. They have focused on Al because of its light weight, ready availability and reactivity with B_4C under reasonable processing conditions.[2] Hence, B_4C–Al composites have the potential to combine the high stiffness and hardness of B_4C with the ductility of Al without defeating the goal of obtaining a strong low-density material. Infiltration of Al into porous monolithic B_4C compacts under an inert atmosphere has been of interest as a cost effective method to produce B_4C–Al composites.[3–6]

Commercially available boron carbide is generally a mixture of B_4C (20 at.% C) and $B_{13}C_2$ (13.8 at.% C).[2] These boron carbides react strongly with Al, resulting in a variety of binary and ternary compounds, including Al_3BC, $AlB_{24}C_4$ (commonly designated as AlB_{10}), $Al_8B_4C_7$, $Al_3B_{48}C_2$ (often known as β-AlB_{12}), AlB_2, $AlB_{12}C_2$, $AlB_{48}C_2$, Al_4C_3 and α-AlB_{12}.[7] However, by shifting the boron carbide composition to the limit of the boron carbide's solid solution range at the carbon-rich end, the kinetics of the boron carbide–Al reaction and types of reactions are drastically changed.[2] Thus, at a temperature range of 900 to 1225 °C, carbon-rich boron carbide reacts with Al, forming principally $AlB_{12}C_2$ and Al_3BC, rather than a multitude of phases. Halverson et al.[8] state that Al_3BC is replaced by other Al–B–C compounds richer in boron ($AlB_{24}C_2$, $AlB_{12}C_2$) and Al–C compounds (Al_4C_3) when infiltrated at higher temperatures and/or applied a post-heat treatment.

* Corresponding author.
E-mail address: garslan@anadolu.edu.tr (G. Arslan).

0955-2219/03/$ - see front matter
PII: S0955-2219(02)00304-7

AlB_2 formation disappears at relatively higher temperatures.

The formation of new ceramic phases increases ceramic phase continuity and thus reduces the toughness. Out of all these ceramic phases, the least detrimental one to toughness is AlB_2. Hardness is found to decline in the order of B_4C, $AlB_{24}C_4$; Al_4BC; AlB_2 and Al. All the new ceramic phases tend to form large clusters of grains and result in lower strength regardless of which phase forms. Therefore, the post-densification heat treatment is recommended only when improvements in hardness and elastic modulus are most critical.[9]

The phase composition in B_4C–Al composites depends on the starting material[7] and processing variables such as (i) thermal or chemical treatment of boron carbide prior to metal infiltration, (ii) the densification temperature and time and (iii) the post-densification heat treatment process.[9] The thermal or chemical treatment causes surface passivation, by changing the surface boron type or carbon/boron ratio that slows down the chemical reactions.[2,5,6] In all cases, the post-densification heat treatment reduces the total amount of unreacted metal. However, this reduction is less in thermally passivated boron carbide[9].

In the work of Pyzik and Beaman,[9] B_4C–Al composites were processed near the melting point of Al, to suppress the low-temperature phases and prevent the formation of high-temperature phases, and then subsequently heat-treated at different temperatures. Their work showed that the reaction between B_4C and Al starts at about 450 °C with the formation of Al_4BC. Above 600 °C, AlB_2 forms and Al is rapidly depleted. Between 600 and 700 °C, AlB_2 and B_4C are the predominant phases. Above 700 °C, AlB_2 and Al_4BC are both present and the relative amount of Al_4BC increases with increasing temperature. Between 900 and 1000 °C, the predominant reaction product is Al_4BC. At about 1000 °C, AlB_2 decomposes and generates free Al. Heat treatment above 1000 °C produces mainly $AlB_{24}C_4$ and small amount of Al_4C_3.

The reactivity data suggest two predominant mechanisms of B_4C and metal depletion in B_4C–Al composites.[9] Phases formed below 1000 °C are Al-rich and their formation leads to the rapid depletion of metal whereas phases formed above 1000 °C are rich in boron and carbon, resulting in B_4C depletion and composites with a large amount of free metal and a small amount of B_4C.

The primary aim of the present work was to systematically characterise the evolution of phases in B_4C–Al composites as a function of processing parameters and to shed light on the wetting mechanism.

2. Experimental

B_4C–Al composites were produced by melt infiltrating 2024 Al alloy blocks into porous B_4C preforms under an Ar atmosphere. The preforms were prepared by pressing three different starting B_4C powders with d_{50} values of 2.6 μm (grade HP, H. C. Starck, Goslar, Germany), 4.7 μm (grade 15, H. C. Starck, Goslar, Germany) and 47 μm (refractory grade, Alfa Aesar, Karlsruhe, Germany). Infiltration temperatures were chosen as 985, 1080, 1180, 1275 and 1370 °C. Heating and cooling rates were 20 °C/min.

Porous B_4C compacts with green densities in the range of 50–70% were prepared by uniaxially pressing starting B_4C powders at 20 MPa pressure. Coating the B_4C powder surfaces with an amorphous SiO_2 layer was also investigated as an alternative method to control the reaction kinetics between B_4C and Al. Fine grained amorphous SiO_2 was derived by hydrolysis of tetraethylorthosilicate ($Si(OC_2H_5)_4$, Merck, Hohenbrunn, Germany) in an ammonium hydroxide (NH_4OH, Merck, Darmstadt, Germany) solution at pH = 12–13 and 2-propanol ($CH_3CH(OH)CH_3$, Merck, Darmstadt, Germany). The molar ratio of $Si(OC_2H_5)_4$:$CH_3CH(OH)CH_3$:NH_4OH was 1:20:30.[10] The SiO_2-coated B_4C powders were prepared with a ratio of 90 B_4C/10 SiO_2 (wt.%).

Passivation of starting B_4C powders was achieved by heat-treating them in the absence of free carbon at 1425 °C for 2 h under an Ar atmosphere prior to the infiltration process.[6]

X-ray diffraction (Rigaku Rint 2200, Tokyo, Japan) was performed using monochromatic CuK_α radiation ($\lambda = 1.5406$ Å). Scanning speed was 1°/min for 2θ, divergence and scattering slit widths were set as 1° while the receiving slit width was set as 0.30 mm. Pure Si powder (99.99% pure, Fluka, Buchs, Switzerland) was used as an internal standard.

Phase quantification was performed by the ratio of slopes method.[11] Reference lines for the pure phases of Al, B_4C and AlB_2 were obtained by X-raying mixtures of at least three different known weight ratios of pure phase to Si. For each data point, the average of the three values obtained for the intensity ratios were plotted against the value of the weight ratio of the pure phase to the standard. After determining the slopes of the reference lines, the slopes of the analysis lines were established in a similar way, but the samples to be X-rayed were mixtures consisting of various proportions of composite powder mixture and Si. The slopes depended on the phase, the chosen peak, the concentration of the phase in the mixture and the selected peak of the internal standard. The content of each phase was obtained by dividing the slope of the analysis line by the respective slope of the reference line. The peak areas were determined from the chart by multiplying peak heights, after accounting for the background, by the peak widths at half the peak heights. The intensity ratios were obtained by dividing the peak areas by the area of the Si peak. The d-spacing of the selected peaks for the phases Al, B_4C, AlB_2 and Si were 2.34, 2.56, 2.60

and 3.14 Å, respectively. Due to the unavailability of single phase of Al_3BC, its amount was obtained indirectly by subtracting the total amount of Al, B_4C and AlB_2 from 100%.

Precise weighing and the ability to use various weight ratios can give this method greater accuracy than that of the classic internal standard method. The weight of the mixture to be analysed, the reference material and the internal standard need not be any specific values or in any fixed proportions. Hence, with the ratio of slopes method one is able to choose weight ratios for which the intensities of the required peaks can be measured accurately.[11]

Another widely recognised method to accurately determine the crystalline phases content is the Rietveld method. In this method, the least-squares refinements are carried out until the best fit is obtained between the entire observed powder diffraction pattern taken as a whole and the entire calculated pattern based on the simultaneously refined models for the crystal structure(s). But, since this method is a structure refinement method and not a structure solution method, per se, a reasonably good structure model for each of the phases to be determined must be known in advance.[12,13]

Microstructural studies of the composites were performed with a scanning electron microscope (CamScan S4, Cambridge, England) attached with an energy dispersive X-ray spectrometer (EDX, Link ISIS 300, Oxford, England).

3. Experimental results and discussion

3.1. Bulk density

B_4C preforms (7 mm thickness) with 2.6 μm average particle size were able to be fully infiltrated at temperatures as low as 1035 °C whereas those with 4.7 μm average particle size required a temperature of at least 1225 °C for full infiltration (holding time 10 min). The bulk densities of most of the B_4C–Al composites—as determined by the Archimedes method—were over 98% of theoretical.[14]

3.2. Quantification method

The weights, weight ratios and average intensity ratios for each of the selected peaks in each pure phase that was used in establishing the reference lines are given in Table 1 and the reference lines are depicted in Fig. 1. In all cases, the fit parameter (R^2) was found to be greater than 0.98.

The validity of the ratio of slopes method and its accuracy for the B_4C–Al system was verified by quantifying the phases present in two different B_4C–Al powder mixtures of known composition (Table 2). As can be seen from Table 2, the calculated Al content is very close to its real value in both mixtures whereas the accuracy for B_4C content depends to some extent on the composition of the powder mixture. It has a tendency to decrease with increasing Al contents. The accuracy difference in the calculated B_4C and Al contents can be understood if the mass absorption coefficients (μ/ρ) of

Table 1
The weights, weight ratios and intensity ratios for the selected peaks in each pure phase (B_4C, Al and AlB_2) used in establishing the reference lines

Weight (gr)		Weight ratio	Average intensity
Al	Si	(Al/Si)	$Al_{(111)}$ / $Si_{(111)}$
0.3728	0.8866	0.420	0.378
0.7620	0.9948	0.766	0.630
1.4736	0.7503	1.964	1.984
B_4C	Si	(B_4C/Si)	$B_4C_{(104)}$ / $Si_{(111)}$
0.5842	0.3325	1.757	0.158
0.8220	0.2613	3.146	0.221
0.6976	0.1555	4.486	0.346
1.0473	0.2195	4.771	0.387
0.785	0.1385	5.473	0.42
1.4612	0.2128	6.867	0.47
AlB_2	Si	(AlB_2/Si)	$AlB_{2\,(100)}$ / $Si_{(111)}$
0.6115	0.3031	2.018	0.232
0.7682	0.2499	3.040	0.340
0.8676	0.2010	4.018	0.479

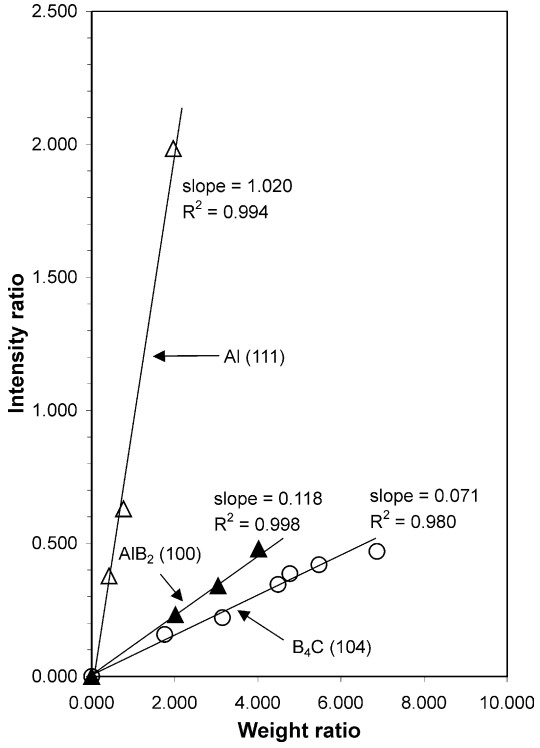

Fig. 1. Reference lines for (104) B_4C, (111) Al and (100) AlB_2 peaks (R^2 denotes the fit parameter of the data points).

Table 2
Comparison of the B_4C and Al contents present in the powder mixtures with those calculated via the ratio of slopes method

Mixture	B_4C and Al content in powder mixture		B_4C and Al content calculated with ratio of slopes method	
	Al (wt.%)	B_4C (wt.%)	Al (wt.%)	B_4C (wt.%)
1	50	50	48.4	43.1
2	20	80	19.5	80.6

the phases are considered. For CuK_α radiation, μ/ρ of the phases Al, B_4C and Si (standard) are 50.23, 2.88 (estimated by using the rule of mixtures) and 65.32 cm^2/g, respectively. While the μ/ρ value of Al is close to that of the Si, the μ/ρ value of B_4C is much less than that of Al and Si, implying that the more Al and/or Si is present the more the suppression in intensity of B_4C peaks, which in turn increases the error made in calculating the B_4C peak area.[11] Hence, it is expected that for a given Si content, richer the powder mixture in B_4C, the more accurate the calculated B_4C content. The accuracy of the calculated Al content, on the other hand, is expected to be less sensitive to the composition. Both statements are in good agreement with the data in Table 2. As depicted in Fig. 2, the good correlation between the peak intensities and the amount of the phases provides additional support that the ratio of slopes method has an acceptable accuracy in the quantification of the phases.

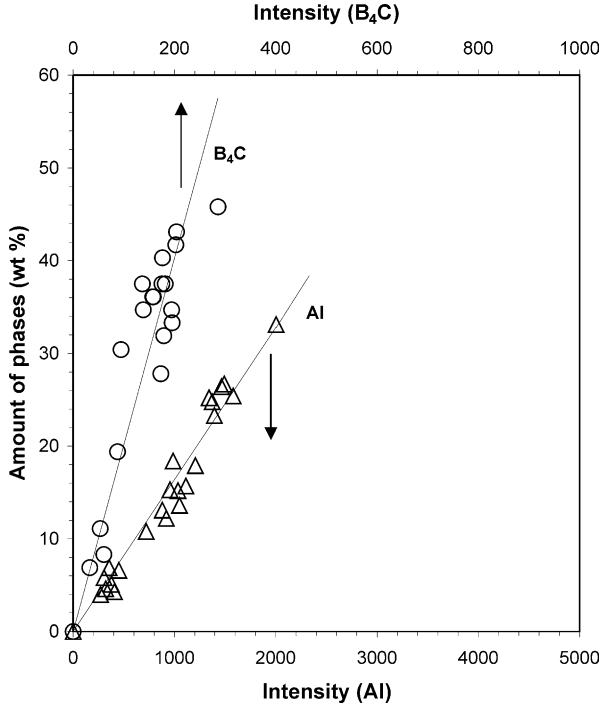

Fig. 2. Relationship between measured phase intensity and calculated phase content for B_4C and Al phases.

3.3. Phases forming and their quantification

The phases and their quantities were systematically analysed in the composites produced from 2.6 and 4.7 μm starting B_4C powders as a function of the infiltration temperature and post- heat treatment. As shown in Figs. 3 and 4, unreacted B_4C and Al and reaction products of Al_3BC and AlB_2 phases are present in all the composites. The amount of reaction products, however, is found to depend on the infiltration conditions (Figs. 5 and 6), as expected.

The $AlB_{12}C_2$ phase starts to form at 1370 °C in the composites produced from 2.6 μm B_4C starting powder when infiltrated for 10 min [Fig. 3(a)] whereas $AlB_{12}C_2$ phase formation is not observed for the composite produced from 4.7 μm B_4C starting powder [Fig. 4(a)]. On applying a post-heat treatment of a 2-h hold at the respective infiltration temperature, the lowest temperature for $AlB_{12}C_2$ formation is shifted from 1370 to 1275 °C for the composite produced from 2.6 μm B_4C starting powder [Fig. 3(b)]. The post-heat treatment also causes $AlB_{12}C_2$ formation to start at and above 1275 °C for the composite produced from 4.7 μm B_4C starting powder [Fig. 4(b)]. Simultaneous inspection of Figs. 3(a) and 5(a), 3(b) and 5(b), and 4(b) and 6(b) reveals that the formation of the boron-rich $AlB_{12}C_2$ phase drastically increases B_4C consumption, causing almost full depletion of the B_4C phase at certain infiltration conditions [Figs. 5(b) and 6(b)].

The Al_4C_3 phase, which is not observed to form for a holding time of 10 min at the investigated temperature interval [Figs. 3(a) and 4(a)], starts to form at the higher end of the investigated temperature range when the holding time at the infiltration temperature is extended to 2 h [Figs. 3(b) and 4(b)]. Its lowest formation temperature is shifted from 1275 to 1370 °C on increasing the average particle size of the B_4C starting powder from 2.6 to 4.7 μm [Figs. 3(b) and 4(b)]. The precipitate $CuAl_2$ forms in all of these composites since an Al-Cu alloy (2024) was used as the metal source.

Extending the holding time to 1 day causes almost full depletion of the initial B_4C content resulting in a further increase in the reaction products while some free Al still remains in the microstructure (Fig. 7).

3.3.1. Al_3BC formation

Quantitative XRD analysis showed that Al_3BC is the main reaction product and its amount varies between 30 and 75 wt.% depending on infiltration conditions and the particle size of the starting B_4C powder [Figs. 5 and 6]. It has a tendency to increase with increasing infiltration temperature until the boron-rich $AlB_{12}C_2$ phase starts to form [Figs. 3(a) and 5(a)]. With the start of formation of this phase, the consumption of B_4C increases drastically [Figs. 3(a), 4(b), 5(a) and 6(b)] and

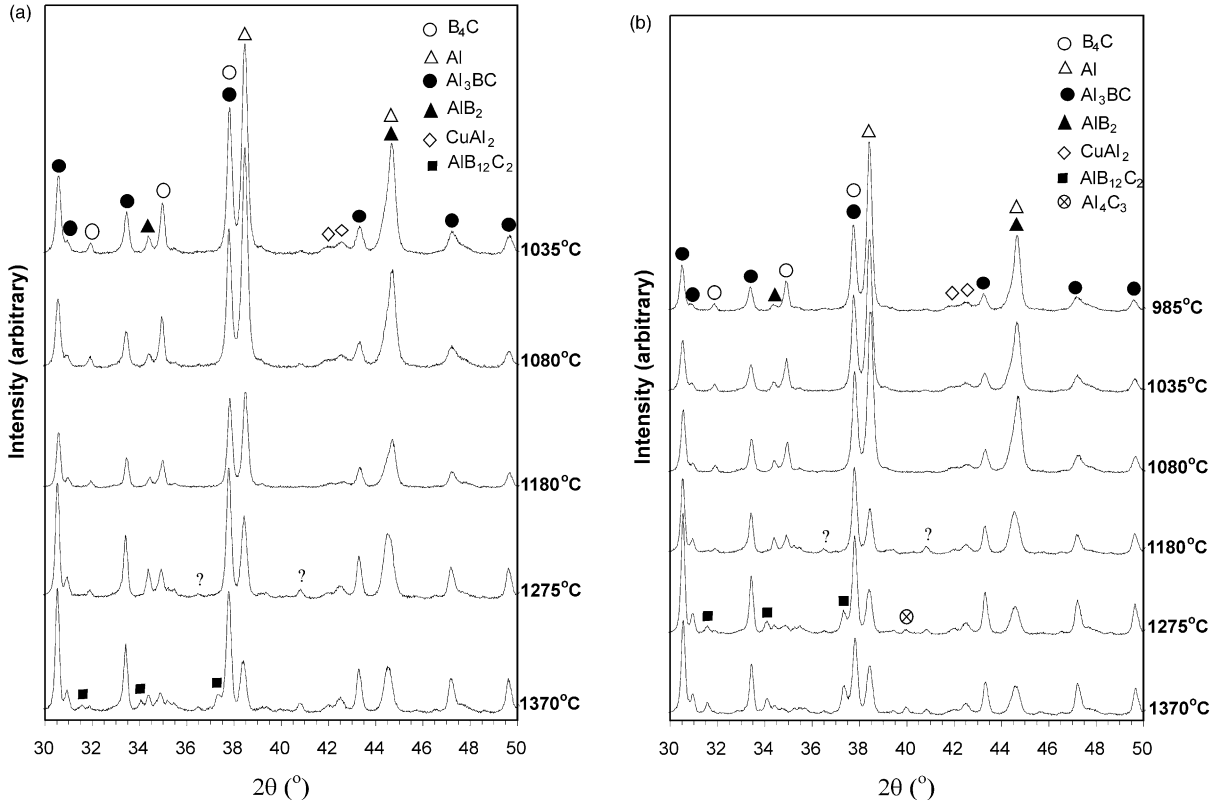

Fig. 3. XRD patterns of B_4C–Al composites prepared from 2.6 μm starting B_4C powders and held at different infiltration temperatures for (a) 10 min and (b) 2 h. Unidentified peaks are indicated with a question mark.

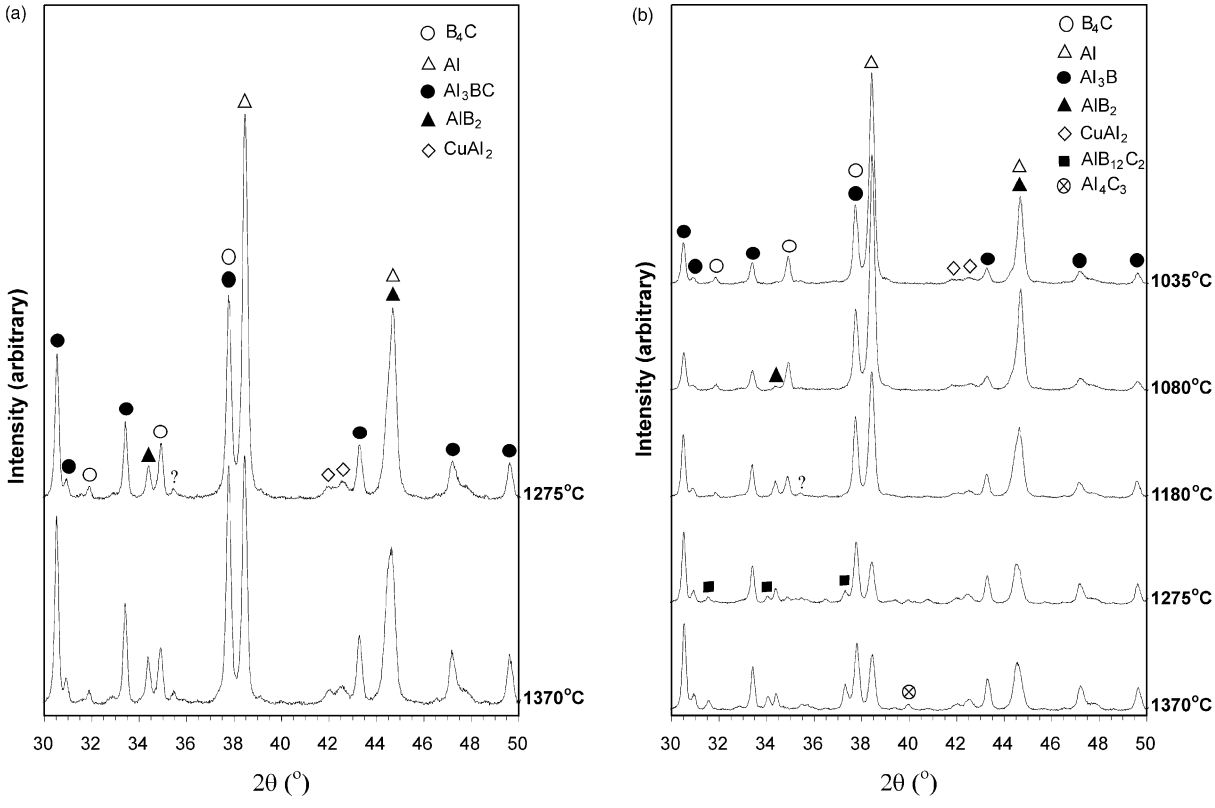

Fig. 4. XRD patterns of B_4C–Al composites prepared from 4.7 μm starting B_4C powders and held at different infiltration temperatures for (a) 10 min and (b) 2 h. Unidentified peaks are indicated with a question mark.

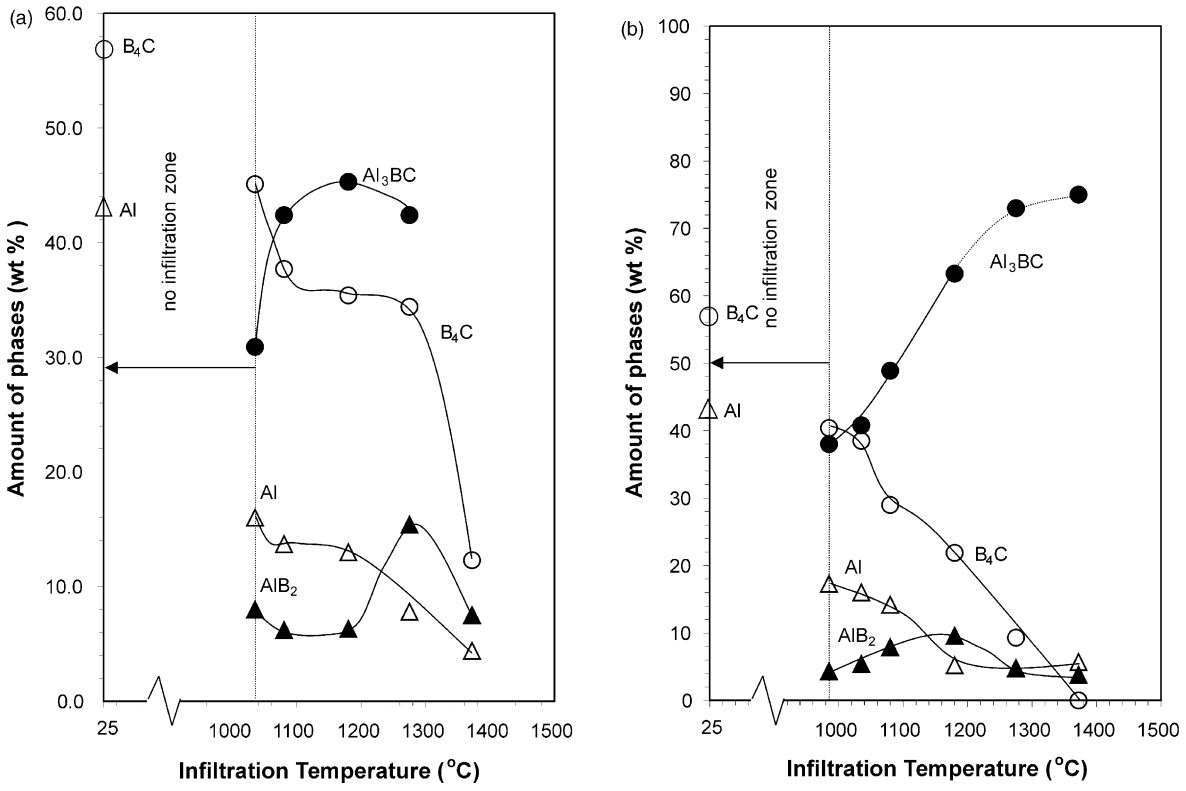

Fig. 5. Calculated phase contents of B_4C–Al composites prepared from 2.6 μm starting B_4C powders held at infiltration temperature for (a) 10 min and (b) 2 h (dashed line indicates estimated Al_3BC content). Initial B_4C and Al contents are 57 and 43 wt.%, respectively.

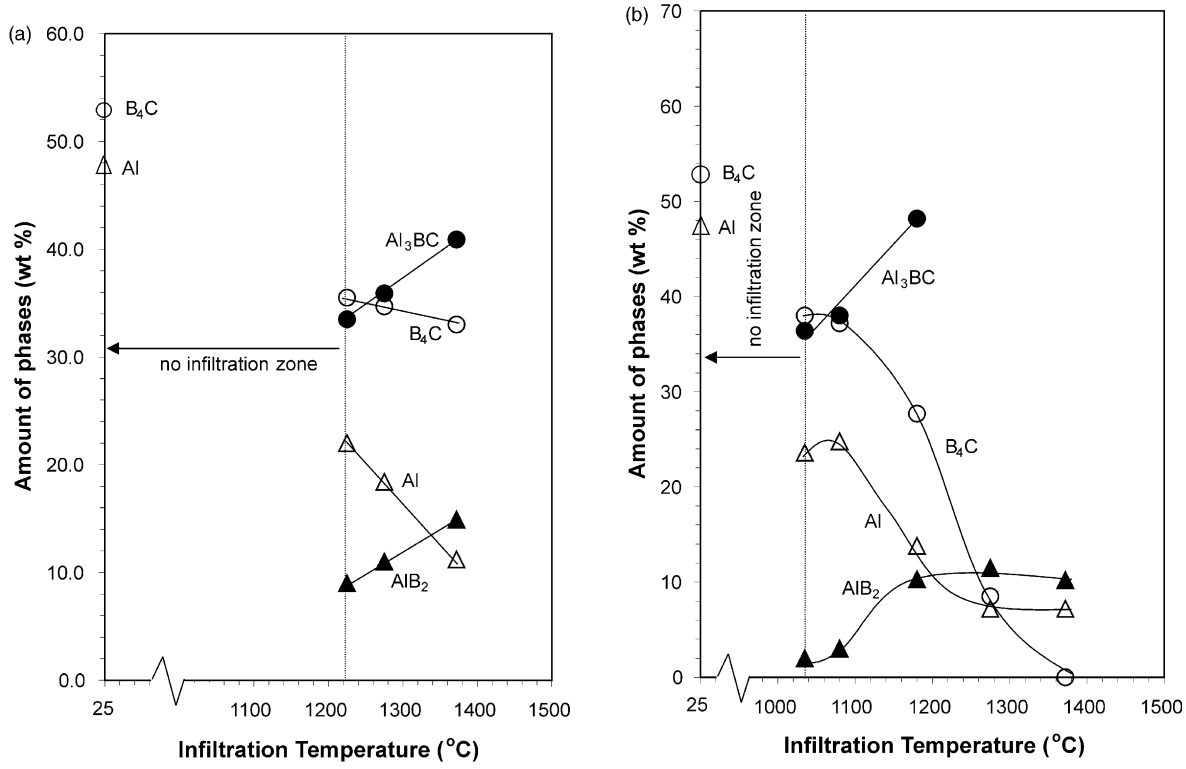

Fig. 6. Calculated phase contents of B_4C–Al composites prepared from 4.7 μm starting B_4C powders held at infiltration temperature for (a) 10 min and (b) 2 h. Initial B_4C and Al contents are 53 and 47 wt.%, respectively.

the amount of the Al-rich Al_3BC phase remains about constant [Fig. 5(a) and (b)], presumably due to the low amount of free metal remaining in the composites (Figs. 5 and 6).

3.3.2. AlB_2 formation

The AlB_2 phase is observed to be generally between 2 and 10 wt.%, but never exceeds 16 wt.% in the investigated temperature and time interval (Figs. 5 and 6). Its amount increases with increasing infiltration temperature until it reaches a maximum. On further increasing the infiltration temperature, the AlB_2 content has a tendency to decline. A post-heat treatment (2-h hold at infiltration temperature) shifts the temperature at which the AlB_2 content reaches its maximum to lower temperatures and decreases the maximum achievable AlB_2 content (Fig. 5). Increasing the particle size of the starting B_4C powders seems to delay this decline stage (Fig. 6). Unlike in composites produced from 2.6 μm B_4C powder, AlB_2 formation is almost completely suppressed in the post-heat treated composites produced from 4.7 μm B_4C powder at infiltration temperatures less than 1180 °C [Figs. 4(b) and 6(b)]. If the XRD patterns of the composites are evaluated with their respective quantified phase contents simultaneously, it is understood that the decline of the AlB_2 content is associated with the formation of $AlB_{12}C_2$ phase. For example, the AlB_2 content in the composite that was produced using 2.6 μm B_4C powder and infiltrated at 1275 °C for 10 min, is about 16 wt.% but decreases to 8 wt.% if the infiltration temperature is raised to 1370 °C [Fig. 5(a)]. While no $AlB_{12}C_2$ formation is detected up to 1275 °C, some $AlB_{12}C_2$ formation is observed at 1370 °C [Fig. 3(a)]. Similarly, for the post-heat treated composites, the AlB_2 content calculated as 10 wt.% at 1180 °C declines to 5 wt.% at 1275 °C and to 4 wt.% at 1370 °C [Fig. 5(b)]. Again, XRD studies do confirm that $AlB_{12}C_2$ forms at 1275 and 1370 °C [Fig. 3(b)].

Similarly, in the composites produced from 4.7 μm B_4C powder (infiltration time 10 min), AlB_2 content is observed to increase steadily with increasing infiltration temperature reaching up to 15 wt.% at 1370 °C [Fig. 6(a)]. No $AlB_{12}C_2$ formation is observed under these processing conditions [Fig. 4(a)]. When the composites were post-heat treated, $AlB_{12}C_2$ formation was detected at and above 1275 °C [Fig. 4(b)]. Although a clear decrease in the AlB_2 content is not observed, its amount remains constant at around 10 wt.% at 1275 °C, [Fig. 6(b)].

3.3.3. Phase evolution during infiltration and cooling steps

For better understanding of the reaction kinetics in the B_4C–Al system, the quantities of the phases present in the composites were identified after the infiltration and cooling processes (Tables 3–6). The phase contents

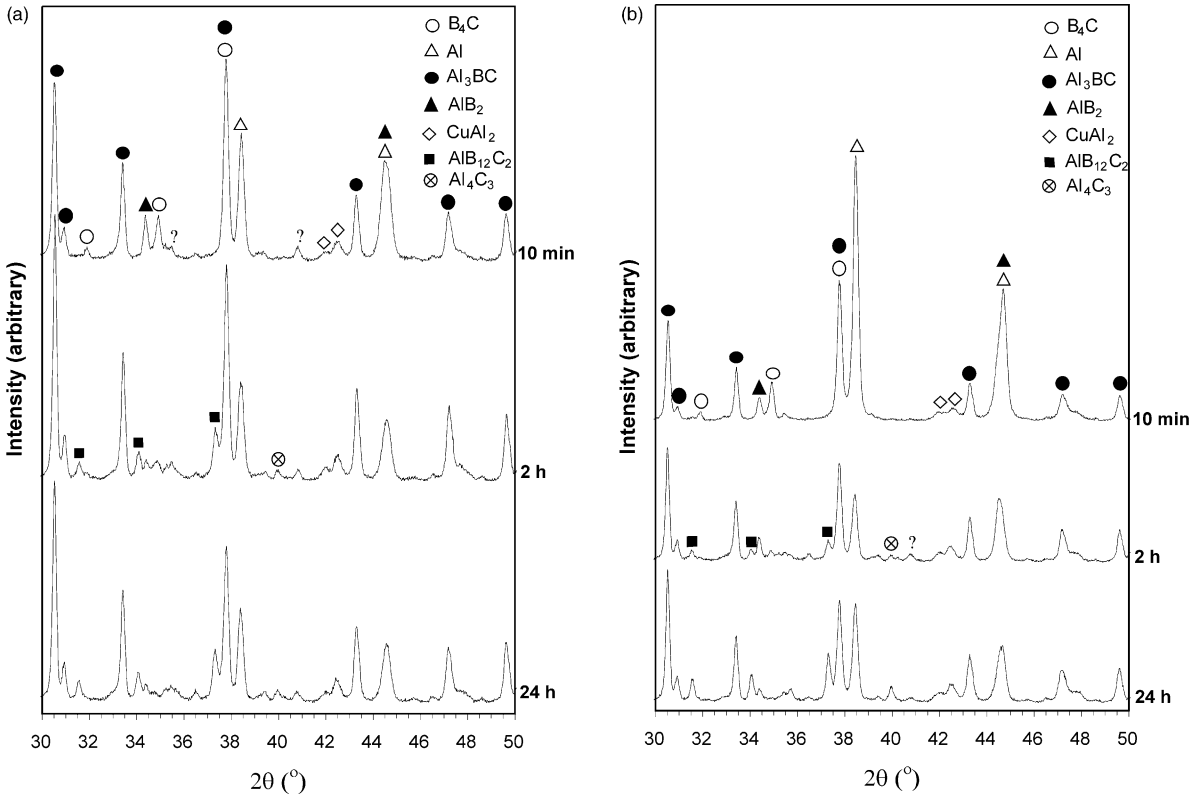

Fig. 7. XRD patterns of B_4C–Al composites as a function of holding time at the infiltration temperature of 1370 °C prepared from (a) 2.6 μm starting B_4C powders and (b) 4.7 μm starting B_4C powders. Unidentified peaks are indicated with a question mark.

Table 3
Phase content (wt.%) of composite after the infiltration and cooling stages that was produced from 2.6 μm B_4C starting powder and infiltrated at 1080 °C for 10 min

	Phases reacting		Phases forming	
	B_4C	Al	Al_3BC	AlB_2
Initial amount	57	43	0	0
Amount after infiltration stage	46	20	32	2
Amount after cooling stage	38	13	43	6
Amount reacting/forming during infiltration stage	11	23	32	Trace
Amount reacting/forming during cooling stage	8	7	11	6
Total amount reacting/forming	19	30	43	6

Table 4
Phase content (wt.%) of composite after the infiltration and cooling stages that was produced from 4.7 μm B_4C starting powder and infiltrated at 1275 °C for 10 min

	Phases reacting		Phases forming	
	B_4C	Al	Al_3BC	AlB_2
Initial amount	53	47	0	0
Amount after infiltration stage	41	27	30	2
Amount after cooling stage	35	18	36	11
Amount reacting/forming during infiltration stage	12	20	30	Trace
Amount reacting/forming during cooling stage	6	9	6	11
Total amount reacting/forming	18	29	36	11

just after the infiltration process were approximated by very fast cooling the metal infiltrated porous B_4C compacts from the infiltration temperature down to 400 °C within 2 min.

For example, when the composite produced by infiltrating 57% dense preforms of 2.6 μm B_4C starting powder with Al at 1080 °C for 10 min was cooled at the standard rate of 20 °C/min, the Al and B_4C contents were measured as 13 and 38 wt.%, respectively (Table 3). Thus, the composite consisted of 51 wt.% unreacted B_4C and Al. When the same composite was cooled at a rate of 400 °C/min, the Al and B_4C contents in the composite were measured to be 20 and 46 wt.%, respectively (Table 3), approximating the composition just after the infiltration process.

Considering 57% density of the preform, the initial amount of Al was 43 wt.% and the total amount of Al reacting was 30 wt.% of which 23 wt.% was consumed during the infiltration stage and 7 wt.% during the cooling stage. Therefore, 70% of the initial Al content reacted with B_4C, and 77% of reacting Al was depleted during the infiltration process (Table 5). Similarly, the initial amount of B_4C was 57 wt.% and the total amount of B_4C reacting was 19 wt.% of which 11 wt.% was consumed during the infiltration stage and 8 wt.% during the cooling stage. Thus, the depletion of B_4C was much less than that of Al since only 33% of the initial B_4C content reacted with Al. 58% of reacting B_4C was depleted during the infiltration process (Table 5).

Table 5
Distribution (%) of phases reacting and forming during the infiltration and cooling stages in the composite that was produced from 2.6 μm B_4C starting powder and infiltrated at 1080 °C for 10 min

Stage	Phases reacting		Phases forming	
	B_4C	Al	Al_3BC	AlB_2
Infiltration	58	77	74	0
Cooling	42	23	26	100

Table 6
Distribution (%) of phases reacting and forming during the infiltration and cooling stages in the composite that was produced from 4.7 μm B_4C starting powder and infiltrated at 1275 °C for 10 min

Stage	Phases reacting		Phases forming	
	B_4C	Al	Al_3BC	AlB_2
Infiltration	67	69	83	0
Cooling	33	31	17	100

The total amount of reaction products forming during the infiltration and cooling processes was 49 wt.%, which was comprised of 43 wt.% Al_3BC and 6 wt.% AlB_2 (Table 3). Accordingly, 88% of the reaction product was Al_3BC. 32 wt.% of Al_3BC and a trace amount of AlB_2 formed during the infiltration stage while 11 wt.% of Al_3BC and 6 wt.% of AlB_2 formed during the

cooling stage. Hence, the amount of Al_3BC forming during the infiltration and cooling stages was determined as 74 and 26%, respectively (Table 5). In contrast, nearly all of the AlB_2 phase formed during the cooling stage (Table 5).

Table 7
Ratios of Al_3BC and AlB_2 to phases forming (PF) during the infiltration and cooling stages of the composites given in Tables 3 and 4

Stage	2.6 μm B_4C powder		4.7 μm B_4C powder	
	Al_3BC/PF	AlB_2/PF	Al_3BC/PF	AlB_2/PF
Infiltration	100	0	100	0
Cooling	65	35	35	65

Table 8
Total amount (wt.%) of starting constituents and reaction products in the composites produced from 2.6 μm B_4C starting powder at different infiltration temperatures and holding times (10 min and 2 h)

Infiltration temperature	Holding time			
	10 min		2 h	
	Starting constituents	Reaction products	Starting constituents	Reaction products
985 °C	No infiltration		58	42
1035 °C	61	39	54	46
1080 °C	52	48	43	57
1180 °C	49	51	27	73
1275 °C	42	58	14	86
1370 °C	17	83	6	94

Table 9
Total amount (wt.%) of starting constituents and reaction products in the composites produced from 4.7 μm B_4C starting powder at different infiltration temperatures and holding times (10 min and 2 h)

Infiltration temperature	Holding time			
	10 min		2 h	
	Starting constituents	Reaction products	Starting constituents	Reaction products
985 °C	No infiltration		No infiltration	
1035 °C	No infiltration		62	38
1080 °C	No infiltration		62	38
1180 °C	No infiltration		42	58
1275 °C	53	47	16	84
1370 °C	44	56	7	93

Table 7 shows that the reaction products formed during the infiltration stage consisted of almost entirely Al_3BC phase, while those that formed during the cooling stage consisted of 65% Al_3BC and 35% AlB_2. The amount of AlB_2 forming during the cooling stage increased with increasing B_4C particle size (Table 7), which could be due to the shift in infiltration temperature with increasing particle size and hence extension in cooling time.

Similar results are obtained for composites produced from 4.7 μm B_4C starting powder that were infiltrated at 1275 °C for 10 min (Tables 4, 6 and 7).

3.3.4. Effect of particle size

Figs. 3 and 4 also show the effect of the particle size of the B_4C starting powders on the reaction kinetics between B_4C and Al. The formation of the boron-rich $AlB_{12}C_2$ phase at 1370 °C is suppressed by increasing the particle size of the starting B_4C powder from 2.6 μm to 4.7 μm [Fig. 3(a)]. Quantitative phase analysis has shown that B_4C–Al composites produced from 4.7 μm B_4C powders are richer in the starting constituents (especially Al) and have less reaction products. For example, at 1275 °C with an infiltration time of 10 min, the B_4C–Al composites produced from 4.7 μm B_4C powder were found to have 53 wt.% starting constituents whereas composites produced from 2.6 μm B_4C powder had only 42 wt.% starting constituents (Tables 8 and 9). By increasing the infiltration temperature to 1370 °C, the starting constituents in the former one decreased from 53 to ≈44 wt.%, while in the latter one they decreased from 42 to ≈17 wt.%. The start of formation of the boron-rich $AlB_{12}C_2$ phase at that temperature [Fig. 3(a)] leads to the formation of a composite that is comprised mainly of reaction products (83 wt.%) and a low amount of free metal content of about 6 wt.% (Table 8).

With the use of an even coarser B_4C starting powder, the reaction kinetics of the system could be reduced even further leading to B_4C–Al composites free of AlB_2 and much reduced Al_3BC contents (Table 10). For example, a 10-fold increase in the d_{50} value of the starting powder from 4.7 to 47 μm decreased the reaction products from about 47 wt.% (Table 9) to 17 wt.% (Table 10), processed under similar infiltration conditions. Unreacted Al content increased from 18 (Table 4) to 35 wt.% (Table 10). Reduction of reaction between

Table 10
Total amount (wt.%) of starting constituents and reaction products in the composites produced from 47 μm B_4C powder, triple mixture and passivated triple mixture at an infiltration temperature of 1225 °C and for 10 min holding time

	Starting constituents			Reaction products		
	B_4C	Al	Total	Al_3BC	AlB_2	Total
47 μm B_4C	48	35	83	17	Trace	17
Triple mixture (d_{50} ≈22 μm)	49	20	69	31	Trace	31
Passivated triple mixture (d_{50} ≈22 μm)	68	26	94	6	Trace	6

B_4C and Al with increasing particle size is due to reduction of surface contact area between B_4C and Al. The SEM-BEI images of these two composites and the EDX spectra of the phases present are depicted in Figs. 8 and 9, respectively. The dark grey particles are B_4C [Fig. 9(a)], the light grey regions show the reaction products [Fig. 9(b)] and the white regions show the Al alloy matrix [Fig. 9(c)]. A comparison of Fig. 8(a) with (b) clearly confirms the reduction in the reacted phases and the enrichment in unreacted B_4C and Al. Furthermore, the metal phase is continuous in the microstructure of the composite produced from 47 μm B_4C starting powder [Fig. 8(b)].

3.3.5. Passivation treatments

Altering the surface chemistry of the chosen starting B_4C powders can control the reactivity between B_4C and Al and thus the amount of reaction products forming. For example, coating the surface of B_4C powders with a homogeneous amorphous SiO_2 layer[15] significantly increased the amount of free Al in the composite from 8 to 22 wt.% (2.6 μm B_4C powder infiltrated at 1275 °C for 10 min, Fig. 10). This indicates that the presence of the homogeneous SiO_2 layer prior to the reaction stage effectively inhibits or retards direct contact of Al with B_4C.

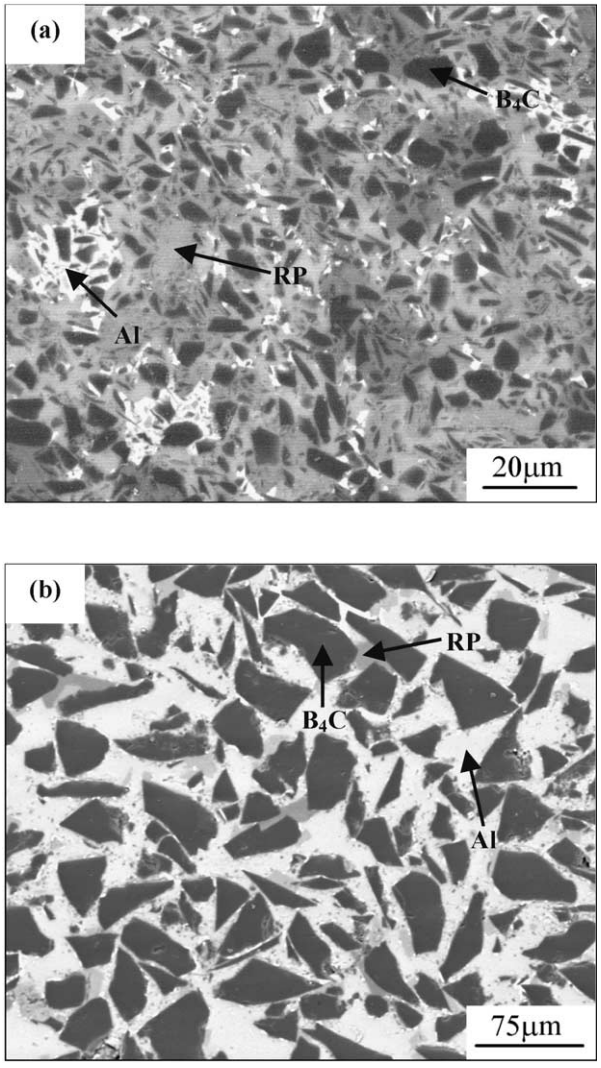

Fig. 8. Backscattered scanning electron microscope images of B_4C–Al composites produced by holding at 1225 °C for 10 min prepared from (a) 4.7 μm starting B_4C powders and (b) 47 μm starting B_4C powders.

Another means of decreasing reactivity is altering the surface chemistry of B_4C powders through a passivation treatment.[6] The least amount of reaction products were established by applying the passivation heat treatment to the porous compact of 70% green density that was produced from the triple B_4C powder mixture. The amounts of starting constituents and reaction products of composites produced from passivated and as-received B_4C powders of 22 μm average particle size (obtained by mixing 2.6, 4.7 and 47 μm powders at the ratio of 5:24:71, respectively) are compared in Table 10. It is observed that the passivation treatment causes the Al content to increase from 20 to 26 wt.% and the unreacted B_4C to increase from 49 to 68 wt.%, which is quite significant. The concomitant decrease in the Al-rich Al_3BC phase from 31 to as low as 6 wt.% is even more pronounced, especially if referred to the increase in Al content, leading to a composite with 94 wt.% starting constituents (Table 10). Fig. 11 illustrates the backscattered SEM image of a B_4C–Al composite prepared from the passivated triple mixture of 2.6, 4.7 and 47 μm B_4C starting powders and infiltrated at 1225 °C for 10 min. Again, the Al alloy matrix is seen as white, the dark grey particles are B_4C and the reaction products are seen as light grey. It is noted that the reaction products mainly form in the vicinity of the finer B_4C particles possibly due to their higher surface area.

3.4. General discussion

Based on the quantification of the phases formed during the infiltration and cooling stages, it is concluded that fast cooling reduces the amount of reacted phases. Particularly, the formation of AlB_2 can be avoided. This indicates that Al_3BC is forming before AlB_2.

The XRD results of the present work are in partial agreement with the literature data.[5,7,9,16] It was confirmed that Al_3BC formation predominates at temperatures exceeding 1000 °C and that only a limited amount of α-AlB_2 forms. The boron-rich phases (α-AlB_{12} and $AlB_{24}C_4$), under the present processing conditions, however, have not been identified to exist in the final microstructure. Nevertheless, according to the Al-B binary phase diagram,[17] α-AlB_{12} might have formed during the infiltration stage. Yet, with increasing Al_3BC contents, a point will be reached where the liquid Al–B solution is enriched in boron due to Al depletion such that no more boron can be dissolved leading to the

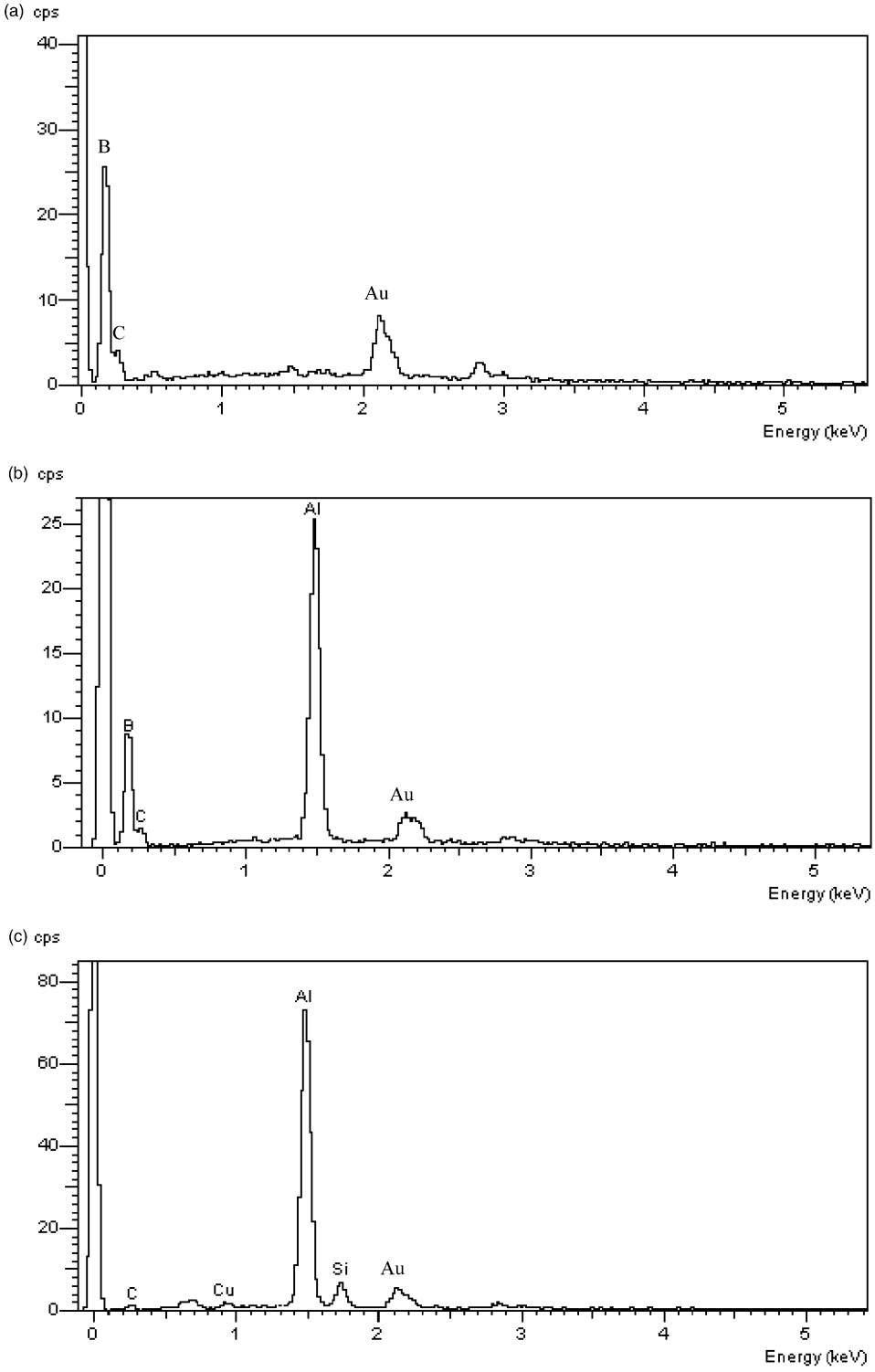

Fig. 9. EDX spectrum of (a) B_4C (b) reaction products (Al_3BC or AlB_2) and (c) Al alloy indicated in Fig. 8.

precipitation of α-AlB_{12}. This α-AlB_{12}, however, should then transform to AlB_2 during cooling. This route of AlB_2 formation, which is based on crystallisation from the Al matrix far away from the B_4C/Al interface,[7] would support the formation of AlB_2 in limited amounts when compared with Al_3BC.

Contrary to the results of Pyzik and Beaman,[9] heat treatments above 1000 °C, did not result in composites with increased Al contents that could be related to the formation of boron-rich reaction products and generation of free Al from the decomposition of AlB_2. One possible explanation is that formation of the boron-rich

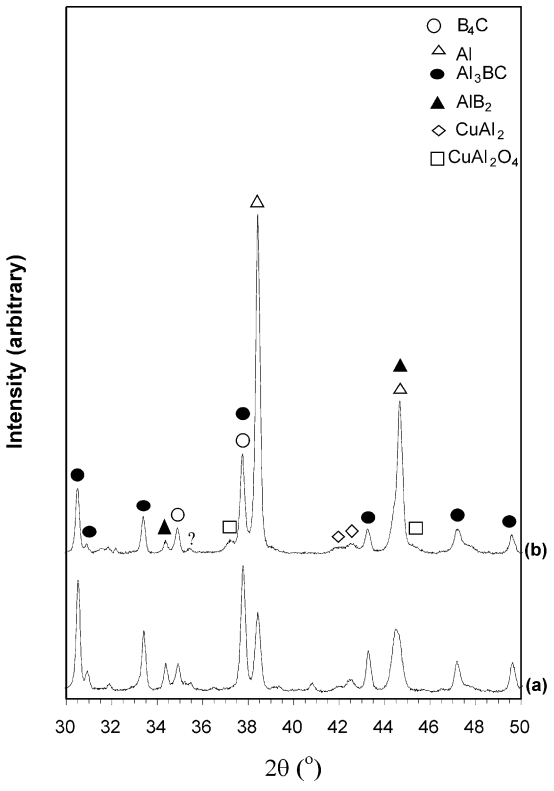

Fig. 10. XRD patterns of B_4C–Al composites prepared from (a) as-received and (b) SiO_2 coated 2.6 μm starting B_4C powders held at 1275 °C for 10 min. Unidentified peaks are indicated with a question mark.

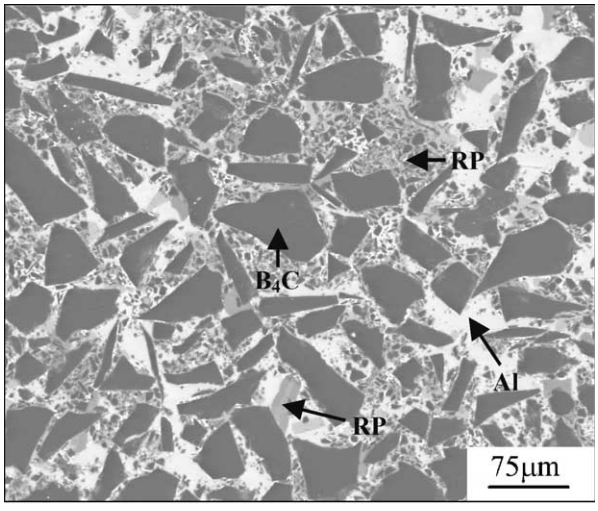

Fig. 11. Backscattered scanning electron microscope image of a B_4C–Al composite prepared from the passivated triple mixture of 2.6, 4.7 and 47 μm B_4C starting powders and infiltrated at 1225 °C for 10 min.

compounds is always preceded by the formation of Al-rich compounds and that the produced composites contain a relatively small amount of AlB_2.

According to the results of the present work, in the temperature range investigated in this study, wetting seems to be associated with the formation of Al_3BC only. AlB_2 is not expected to play a part in wetting. The result of this work is in agreement with that of Viala and Bouix,[7] in which it is stated that B_4C particles are generally surrounded by Al_3BC crystals while AlB_2 crystals are most often embedded in the Al matrix, far away from the B_4C–Al reaction front. It is also in good agreement with the work of Fujii et al.,[16] who did not detect uniformly distributed α-AlB_{12} and AlB_2 crystals throughout the BN–Al interface. Furthermore, boron is not a surfactant of Al[16] implying that Al–B compounds are not expected to play a major role in reactive wetting of B_4C–Al composites.

Although the phase composition of the produced composites is quite different from that of Halverson et al.,[8] the findings are in agreement with their conclusions in that extended heat treatments at 1370 °C resulted in a change in the relative amounts of phases present and also in a change of the chemistry of composites.

4. Conclusions

XRD results showed that B_4C–Al composites produced under the present processing conditions are composed of various combinations of Al_3BC, AlB_2, $AlB_{12}C_2$ and Al_4C_3 phases. The type of phases formed and their quantity depends on processing conditions. By adjusting the processing parameters, the composition of the produced composites can be tailored according to the needs. The amount of reaction products increases with increasing infiltration temperature, increasing infiltration time and decreasing grain size. Either coating the surface of the starting B_4C powder with SiO_2 or passivating it can reduce their amount substantially.

The AlB_2 phase forms at relatively small amounts and its formation can be significantly suppressed or totally eliminated by increasing the particle size of the starting B_4C powder and/or altering its surface chemistry. The Al_3BC phase, on the other hand, is observed to be the main reaction product forming and it is present in all composites. The other phases ($AlB_{12}C_2$ and Al_4C_3) are formed only at the higher end of the investigated temperature interval of 985–1370 °C. With the onset of formation of the boron-rich $AlB_{12}C_2$ phase, the depletion of B_4C increases significantly. The hygroscopic Al_4C_3 phase necessitates a prolonged exposure in addition to high temperatures.

In the investigated temperature range, reactive wetting is associated with the formation of the Al-rich Al_3BC reaction product.

Acknowledgements

The authors would like to thank Anadolu University Research Foundation for funding the present work under a contract number of 990239.

References

1. Thevenot, F., A review on boron carbide. *J. Eur. Ceram. Soc.*, 1990, **6**, 205.
2. Pyzik, A. J. and Aksay, I. A. *Multipurpose boron carbide–aluminium composite and its manufacture via the control of the microstructure*. US Patent No: 4702770, 1987.
3. Pyzik, J. A. and Nilsson, R. T. *B_4C–Al cermets and method for making same*. US Patent No: 5039633, 1991.
4. Gazza, G. E. *Ceramic-metal systems by infiltration*. US Patent No: 3864154, 1975.
5. Halverson, D. C. and Landingham, R. L. *Infiltration processing of boron carbide-, boron-, and boride-reactive metal cermets*. US Patent No: 4718941, 1988.
6. Pyzik, A. J., Deshmukh, U. V., Dummead, S. D., Allen, T. L. and Rossow, H. E. *Light weight boron carbide-aluminium cermets*. US Patent No: 5521016, 1996.
7. Viala, J. C. and Bouix, J., Chemical reactivity of aluminium with boron carbide. *J. Mater. Sci.*, 1997, **32**, 4559.
8. Halverson, D. C., Pyzik, A. J. and Aksay, I. A. *Boron–carbide-aluminium and boron-carbide- reactive metal cermets*. US Patent No: 4605440, 1986.
9. Pyzik, A. J. and Beaman, D. R., Al-B-C phase development and effects on mechanical properties of B_4C/Al-derived composites. *J. Am. Ceram. Soc.*, 1995, **78**, 305.
10. Chen, C. C. and Yen, F. S., Effects of amorphous silica coatings on the sintering behaviours of SiC whisker-reinforced Al_2O_3 composite. *J. Mater. Sci.*, 1994, **29**, 3215.
11. Monshi, A. and Messer, P. F., Ratio of slopes method for quantitative X-ray diffraction analysis. *J. Mater. Sci.*, 1991, **26**, 3623.
12. Krischner, H. and Koppelhuber-Bitschnau, B., *Röntgenstrukturanalyse und Rietveldmethode*. Friedrich Vieweg & Sohn Verlagsgesellschaft mbH, Braunschweig/Wiesbaden, 1994.
13. Young, R. A., Introduction to the rietveld method. In *Int. Union of Crystallography*, ed. R. A. Young. Oxford University Press, New York, 1993, pp. 1.
14. Arslan, G. *Processing and characterization of boron carbide–aluminium composites*. PhD thesis, Anadolu University, Eskisehir, Turkey, 2001.
15. Arslan, G., Kara, F. and Turan, S., Microstructural characterisation of melt infiltrated boron carbide-aluminium composites. *Inst. Phys. Conf. Ser.*, 2001, **168**, 322.
16. Fujii, H., Nakae, H. and Okada, K., Interfacial reaction wetting in the boron nitride/molten aluminium system. *Acta Metall. Mater.*, 1993, **41**, 2963.
17. Duschanek, H. and Rogl, P., The Al–B (aluminum–boron) system. *J. Phase Equil.*, 1994, **15**, 543.